Published in final edited form as:

J Cardiovasc Transl Res. 2017 April ; 10(2): 194–205. doi:10.1007/s12265-017-9733-5.

Fixation of Bovine Pericardium-Based Tissue Biomaterial with Irreversible Chemistry Improves Biochemical and Biomechanical Properties

H. Tam[1], **W. Zhang**[2], **D. Infante**[1], **N. Parchment**[1], **M. Sacks**[2], and **N. Vyavahare**[1]

[1]Department of Bioengineering, Clemson University, Clemson, SC 29634, USA

[2]Department of Biomedical Engineering, University of Texas, Austin, TX, USA

Abstract

Bioprosthetic heart valves (BHVs), derived from glutaraldehyde crosslinked (GLUT) porcine aortic valve leaflets or bovine pericardium (BP), are used to replace defective heart valves. However, valve failure can occur within 12–15 years due to calcification and/or progressive structural degeneration. We present a novel fabrication method that utilizes carbodiimide, neomycin trisulfate, and pentagalloyl glucose crosslinking chemistry (TRI) to better stabilize the extracellular matrix of BP. We demonstrate that TRI-treated BP is more compliant than GLUT-treated BP. GLUT-treated BP exhibited permanent geometric deformation and complete alteration of apparent mechanical properties when subjected to induced static strain. TRI BP, on the other hand, did not exhibit such permanent geometric deformations or significant alterations of apparent mechanical properties. TRI BP also exhibited better resistance to enzymatic degradation in vitro and calcification in vivo when implanted subcutaneously in juvenile rats for up to 30 days.

Keywords

Cardiovascular biomaterial durability; Soft tissue biomechanics; Permanent set; Extracellular matrix stabilization; Structural degradation

Introduction

Bioprosthetic heart valves (BHVs) are used to replace stenotic and regurgitant heart valves [1–3]. BHVs do not require long-term anticoagulant therapy and also have more optimal hemo-dynamics as compared to mechanical heart valves, thus making them the preferred option for valve replacements [1, 4]. BHVs are fabricated out of two types of xenogeneic tissues: (1) porcine aortic valve (PAV) leaflets or (2) bovine pericardium (BP) sheet.

Correspondence to: N. Vyavahare.

Compliance with Ethical Standards

Conflict of Interest There are no disclosures or conflicts of interest with the presented study.

Human Subjects/Informed Consent Statement No human studies were carried out by the authors for this article.

Animal Studies All institutional and national guidelines for the care and use of laboratory animals were followed and approved by the appropriate institutional committees.

BP is the most commonly used material to fabricate BHVs and contains a high amount of layered structural proteins (collagen and elastin with proteoglycans) [5–8]. Selected BP sheets are cut into custom leaflet shapes to fit onto sewing rings to fabricate BHV implants. This process allows BHV tissues to have native heart valve like geometry and structure [1, 2, 9, 10]. All commercially available BHVs currently utilize glutaraldehyde (GLUT) chemistry in fabricating the base biomaterial. However, GLUT crosslinked BHVs experience failure either due to calcification or degeneration of tissue within 12–15 years of use [1–3, 11] and seem to fail faster in younger patients [11]. Therefore, BHVs are less frequently used for patients under 65 years of age.

Calcification has been previously shown to originate at sites of high affinity for calcium deposition such as devitalized cells [12, 13] and damaged ECM components like elastin and collagen [14–16]. Therefore, several anti-calcification technologies have been developed to curb calcification through eliminating cellular debris (alcohol, detergent, or surfactant treatments) [17–20] or improving structural integrity of collagen by reducing aldehyde bonds (thermal annealing and adding diamine chain extenders) [21–26]. However, these treatments have only demonstrated efficacy in delaying the onset of calcification in animal studies [24]. Long-term clinical data is still awaited. Small improvement, if any, in the long-term durability of BHV implant life has been added since the introduction of these technologies [27, 28]. Thirty percent of BHVs have also been found to fail due to degeneration and tearing of tissue at suture points without calcification [28]. There is no clear understanding of the mechanisms of this failure and no treatments are proposed to prevent tissue degeneration.

Previous literature suggests that tissue degradation resulting in mechanical failure of BHVs initiates with collagen fiber disruption that is exacerbated over time that results in stress concentrations forming at weak points in BHV design [29, 30]. These stress concentrations, over time, eventually result in tearing causing catastrophic failure [5, 29–31]. Fiber disruption, orientation changes, fatigue-induced fiber damage, and degenerative changes to apparent mechanical properties have previously been found to correlate with ECM component loss such as GAG leeching [32] and elastin degeneration [33–35]. Most recently, it has also been shown that oxidative stress may also play a significant role in BHV leaflet structural degradation [36].

Furthermore, the instability of GLUT crosslinking allows GLUT-treated biomaterials to undergo a phenomenon called “permanent set” described as permanent geometric deformations produced over time due to mechanical insult [5, 6, 30, 31, 37]. Such permanent set effects could drastically increase chances of premature failure of BHVs because permanent set could lead to development of stress concentrations that can result in tearing [5, 31].

In this study, we examined the effect of replacing GLUT with an alternative, irreversible carbodiimide-based crosslinking chemistry (TRI) on tissue properties in an effort to curb both calcification and tissue degeneration failure modes in BHVs. We show that TRI crosslinking provides protection against calcification similar to other anti-calcification methods but more importantly stabilizes more of the ECM of the tissue and produces

stronger and more compliant tissue that does not cause permanent deformation under static strain and resists enzymatic degradation. We hypothesize that such a material would also prevent structural degeneration of BHV implants due to mechanically induced damage in addition to calcification.

Materials and Methods

Fabrication of Tissue-Based Biomaterials

Bovine pericardium (BP) was sourced from a third party abattoir, delivered on 0.9% saline and ice to the laboratory within 24 h of slaughter. BP sacs were cut into flat sheets and were washed in 0.9% saline for 15 min. BP sheets were then treated with two different chemical treatment techniques: (1) GLUT control and (2) TRI novel, more irreversible crosslinking technique. Figure 1 illustrates the fundamental differences between the two methods of chemical crosslinking methods.

GLUT—BP sheets were treated with 0.6% glutaraldehyde in 50 mM 4-(2-hydroxyethyl)-1-piperazineethanesulfonic acid (HEPES)-buffered saline (pH 7.4) at room temperature with gentle shaking for 24 h, solution decanted, and replaced with 0.2% glutaraldehyde in 50 mM HEPES-buffered saline (pH 7.4), and the crosslinking was continued for at least 6 days.

TRI—BP sheets were treated with 0.5 mM neomycin trisulfate solution in 2-(*N*-morpholino) ethanesulfonic acid (MES) buffer for 1 h. The solution was decanted and leaflets were then incubated in a 30 mM 1-*ethyl*-3-(3-dimethylaminopropyl) carbodiimide (EDC) and 6 mM *N*-hydroxysuccinimide (NHS)/0.05% PGG solution in 50 mM MES-buffered saline (pH 5.5) for 24 h. The solution was decanted and then the leaflets were then crosslinked further in 30 mM EDC and 6 mM NHS solution in 50 mM MES-buffered saline (pH 5.5) for 24 h. Following fixation, valves were placed in 20% isopropanol in 50 mM HEPES buffer (pH 7.4) for at least 6 days.

Differential Scanning Calorimetry

Differential scanning calorimetry (DSC) was used to measure the thermal denaturation temperature (T_d) of collagen. Samples (3–8 mg) from each of the TRI and GLUT groups were blotted to remove surface water and placed flat in hermetically sealed DSC aluminum pans. Samples were tested using a DSC 2920 (TA Instruments, Newcastle, DE). A pilot run verified the T_d range for GLUT compared to previous results, and the remainder of samples were equilibrated at 20 °C and heated at 10 °C/min. The denaturation temperature was recorded as the maximum value of the endotherm peak.

Resistance to Enzymatic Treatment

Resistance to Collagenase and Elastase—BP sheets were cut into 1 × 1 cm patches, rinsed in nanofiltered water, blotted dry, frozen, lyophilized, and weighed. BP patches were incubated in 1.2 mL of 5 U/mL porcine pancreatic elastase (Elastin Products Co. Inc., Owensville, MO) in 100 mM Tris, 1 mM $CaCl_2$, 0.02% NaN_3 (pH 7.8) for 24 h, or 75 U/mL collagenase (Type VII, Sigma, St. Louis, MO) in 50 mM Tris, 10 mM $CaCl_2$, and 0.02% NaN_3 (pH 8.0) for 48 h at 37 °C while shaking at 650 RPM. Enzyme liquid was saved for

further studies and digested BP patches were rinsed in nanofiltered water, blotted dry, frozen, lyophilized, and weighed. Percent weight loss was calculated. For storage studies, samples were stored for 60 days in 0.2% glutaraldehyde solution (GLUT samples) or 20% isopropanol in HEPES buffer (TRI samples), taken out of storage, washed in saline ×3 for 15 min, and challenged with the aforementioned protocol with collagenase or elastase and percent weight loss calculated.

Resistance to GAGases—BP sheets were cut into 1 × 1 cm patches and thoroughly washed in 100 mM ammonium acetate buffer (AAB) at pH 7.0 ×3 for 5 min. BP patches were incubated in 1.2 mL GAG-degrading enzyme solution (5 U/mL hyaluronidase (Sigma, St. Louis, MO) and 0.1 U/mL chondroitinase (Sigma, St. Louis, MO) in 100 mM AAB; pH 7.0) or in AAB. Samples were shaken vigorously for 24 h at 37 °C. Following a 24-h incubation, BP patches were washed in distilled water ×3 for 5 min, frozen, and lyophilized. Total hexosamine content was measured using the hexosamine assay as previously reported [38]. Elson and Morgan's modified hexosamine assay was used to measure GAG-related hexosamines. Lyophilized GAG-digested samples were weighed, digested in 2 mL 6 N HCl (24 h, 96 °C), and dried under nitrogen gas. Samples were resuspended in 2 mL 1 M sodium chloride and reacted with 2 mL of 3% acetyl acetone in a 1.25-M sodium carbonate. Ethanol (4 mL) and Ehrlich's reagent (2 mL, 0.18 M *p*-dimethylaminobenzaldehyde in 50% ethanol containing 3 N HCl) were added, and solutions left for 45 min to allow the color to develop. A pinkish-red color is indicative of tissue hexosamine quantities, and the absorbance was read at 540 nm. A set of D (+)-glucosamine standards were used. For storage studies, samples were stored for 21, 60, or 180 days in 0.2% glutaraldehyde solution (GLUT samples) or 20% isopropanol in HEPES buffer (TRI samples) taken out of storage, washed in saline ×3 for 15 min, taken out of storage, and challenged with the aforementioned protocol with collagenase or elastase and percent weight loss calculated.

Suture Pull-Out Test

BP patches were evaluated for structural integrity and its ability to resist tearing. Thick (0.50 mm) sections of patches were used for testing. GLUT and TRI BP patches were cut with a die in rectangular 40 × 4.0-mm sections. Sections were then treated with collagenase, GAGase (combination of enzymes to degrade GAGs), porcine pancreatic elastases, or no enzyme treatment (8 groups, $n = 8$ per group). One side of tissue samples was attached to a bottom clamp in a tensile tester (MTS, Minneapolis, MN). A single suture (Polypropylene blue monofilament 4-0 P-3 Ethicon™, San Lorenzo, Puerto Rico) was pierced through the sample a third of the way down the sample and was clamped to the top clamp. Samples were tensile tested at 12 mm/min to determine the amount of force it took to pull the suture out of the sample. With the peak load, thickness of the sample and width were used to calculate cross-sectional area to determine stress.

Mechanical Characterization

We presorted the native BP using the pSFDI technique [39] to determine the direction of collagen fiber alignment. The specimens were cut so that the preferred direction (PD) of the collagen fibers and cross-preferred direction (XD) are aligned to the two testing axes. Similarly, the mechanical properties before and after static strain were determined using a

custom-built biaxial testing device [40] and analyzed using a method presented in Zhang et al. [41]. TRI or GLUT BP patches were cut into a 20 × 20-mm^2 for mechanical characterization. A maximum load of 1000 kPa was used during testing to ensure all collagen fiber crimping were straightened. Each specimen was first precondition under equibiaxial stress for 15 cycles each with a duration of 16 s. The specimens were tested for eight continuous cycles with different loading ratios (1:4, 1:2, 1:1, 2:1, and 4:1) with the last one taken as representative.

Permanent Set Through Static Strain Test

To accelerate permanent geometric deformation, each patch was loaded into a custom clamp system that held the patch in a static strain position at 20% stretch past nominal length in either the PD (along the collagen fiber alignment) or XD (orthogonal to the collagen fiber alignment) direction. The testing was done at 37 °C and immersed in phosphate-buffered saline. This method was used because it was the simplest way to accelerate permanent set and to test resistance to geometric deformations. After 28 days of static stretch, the change in length was determined in both the PD and XD direction. The change in geometry that occurred was determined using four fiducial markers attached to the center of the specimen [42]. Three specimens were tested with PD alignment for mounting and seven specimens for the XD alignment for GLUT. Five specimens were tested for PD alignment and three specimens were tested for XD alignment for TRI. For each of these alignment groups, the change in length in the PD and XD direction was determined.

Free Amine Content Assay

The primary amine group concentration of tissue samples was determined using a colorimetric assay previously used to study carbodiimide crosslinking [43, 44]. GLUT or TRI BP patches were exposed to a solution of $NaHCO_3$ (2 wt%, pH 9.0, Aldrich, The Netherlands) and 2,4,6 trinitrobenzene sulfonic acid, TNBS (0.5 wt% Fluka, Switzerland). The reaction was continued for 4 h at 40 °C, after which the samples were rinsed in saline solution using a vortex mixer to remove unreacted TNBS.

Samples were freeze-dried overnight, after which the dry mass was determined. Dry samples were immersed in aqueous hydrochloric acid (2 mL, 6 M, and 80 °C; Aldrich, Zwijndrecht, The Netherlands) until fully dissolved. The obtained solution was then diluted with deionized water (8 mL) and the absorbance was measured at 340 nm (Perkin Elmer, Fullerton, USA). The concentration of free amine groups was calculated using the following equation:

$$[NH_2] = \frac{A \cdot V}{\varepsilon \cdot \ell \cdot m_{tissue}}$$

NH_2	Free amine group content	[mol/g of tissue]
A	Absorbance	[unitless]
V	Solution volume	[mL]

ε	14,600	[mL/mmol cm]
ℓ	Path length	[cm]
m_{tissue}	Dry weight of sample	[mg]

The obtained values were used to calculate percent change in free amine content before and after stretch testing.

In Vivo Calcification Model

Following fixation, all tissues were rinsed thoroughly three times in 30 s washes of sterile saline and remained in sterile saline until implantation. Male juvenile Sprague-Dawley rats were anesthetized by inhalation of 3% isoflurane gas. A dorsal surgical incision was made, and two subdermal pockets created on either side of the sagittal plane. Two BP patches (1 ×1 cm) were blotted and positioned to lie as flat as possible in each of the pockets. One sample was placed per pocket. Incisions were closed with surgical staples and samples with fibrous capsule still intact were retrieved after 30 days' implantation. The BP patches and surrounding capsule were removed from the subdermal sites. The middle section was saved for histological analysis. The remaining sections were placed immediately on dry ice and frozen at −80 °C as soon as possible. Clemson University Animal Research Committee approves all animal use protocols (AUP) for the experimental models. All animals receive humane care in compliance with NIH publication no. 86-23, revised in October 2002.

Mineral Analyses

Half samples (without the capsule) from subdermal implantation studies were frozen, lyophilized, weighed, and acid hydrolyzed in 2 mL 6N Ultrex II HCl for 20 h at 96 °C. Samples were dried under nitrogen gas, re-suspended in 1 mL 6N Ultrex II HCl, and centrifuged at high speeds to separate any remaining particles. Samples were diluted 1:50 in nano-filtered water. Calcium and phosphorous content in samples were analyzed using the Spectro Acros ICP Spectrometer (SPECTRO Analytical Instruments, Kleve, Germany). Dilution ratios were used to calculate element content of the sample, and values were normalized to dry sample weight.

Histology

BP sections were cut, stored in formalin, processed, embedded in paraffin, and sectioned at 6 μm for light microscopy analysis. A combined staining technique, Verhoeff's elastic Masson's trichrome method, was utilized to visualize and assess ECM morphology (elastin and collagen) after in vitro enzymatic treatment. Dahl's alizarin red stain with light green counterstain was used to visualize calcium deposition after samples were implanted in vivo; calcium deposits appear red.

Statistical Analysis

Results are expressed as means ± standard errors. Statistical analysis was performed using one-way analysis of variance (ANOVA). Differences between means were determined using the least significant difference with an alpha value of 0.05.

Results

Tissue Crosslinking Assessment

We determined the thermal denaturation temperatures (T_d) of the tissue with DSC. T_d has been shown to effectively correlate with tissue collagen stabilization [32]. Both GLUT- and TRI-treated BP showed adequate increase in T_d (88.08 ± 0.225 or 88.09 ± 0.488 °C, respectively, compared to fresh tissue 56 ± 3.2 °C [32]), suggesting complete collagen stabilization.

Enzyme Stability Studies

After GLUT- or TRI-treated BP was challenged with type I collagenase, no significant difference was detected between GLUT- and TRI-treated BP (2.01% ± 0.726 or 2.94% ± 0.104 mass loss, respectively, $p < 0.0943$) indicating that collagen within the BP was adequately protected from simulated enzymatic degradation in both crosslinking methods (Fig. 2). When GLUT- or TRI-treated BP was challenged with porcine pancreatic elastase, a significant difference was found (8.38% ± 0.520 vs. 4.69% ± 0.491 mass loss, respectively, $p < 0.0002$) indicating that elastin within BP was better protected in TRI-treated BP (Fig. 2). When GLUT- or TRI-treated BP was challenged with a GAGase enzyme cocktail, there was a significant decrease in percent GAGs retained between before buffer/GAGase treatment and after buffer-treated (control group)/GAGase-treated (enzymatic group) GLUT BP samples (59.0% ± 11.35 and 83.0% ± 5.78, respectively). TRI BP groups exhibited no significant percent loss between groups in buffer or GAGase treatment.

We next determined the storage stability of GLUT- or TRI-treated BP patches stored in 0.2% GLUT or 20% isopropanol, respectively (60 days). When GLUT or TRI BP was challenged with collagenase after 60 days of storage, both did not exhibit any detectable mass loss at either time point from $t = 0$ days. However, when GLUT BP was challenged with elastase after 60 days of storage, degradation of elastin was noted by the absence of dark, purple fibrous network (Fig. 3c) that was present before storage (Fig. 3a). Elastase treatment or storage for long periods of time also seemed to alter the collagen structure as noted in the different color of the staining. TRI BP retained the dark purple, black elastin fibrous network after long-term storage with enzymatic challenge (Fig. 3d) compared to before storage (Fig. 3b).

Resistance to Tearing

A suture pull-out test was used to evaluate the biomaterial's ability to resist tearing. Before enzymatic treatment with collagenase, GAGase, or elastase, GLUT BP took significantly less peak stress to cause rupture than TRI BP (2943.5 ± 170.27 and 4689.7 ± 201.00 kPa, respectively, Fig. 4). This data suggests that the TRI treatment protocol produced an inherently more stronger material due to the difference in chemistry. Across all enzymatic treatment groups, GLUT-treated BP exhibited significantly less peak stress to cause rupture than TRI-treated BP. However within GLUT- or TRI-treated BP, enzymatic challenges produced no significant changes in peak stress to cause rupture when compared with the no enzymatic treatment group. There was a noted trend of decreased stress to cause suture

rupture between untreated GLUT BP and collagenase-treated GLUT BP, however, it did not reach statistical significance ($p < 0.133$).

Permanent Set Caused by Induced Static Strain

Data from the static stretch test shows that significant permanent set has occurred after 28 days for GLUT BP but not for TRI BP (Fig. 5 and Table 1). Ideal retention of native geometry indicative of no permanent set effects is represented by a λ of 1 (no change in length). Additionally, permanent set was not found to be dependent on which direction the samples were loaded in. This suggests that permanent set is a crosslinking dependent effect (Table 1).

Biaxial Tensile Testing Before and After Static Stretch Test

Biaxial tensile testing of tissues after crosslinking showed that TRI BP was more compliant than GLUT BP in both the preferred (PD) and nonpreferred (XD) orientations (Fig. 6). In fact, TRI-treated tissues behaved almost similar to native uncrosslinked tissues. Both tissues exhibited nonlinear biomechanical behavior indicative of soft connective tissues before induced static strain with a marked toe region. After induced static strain, GLUT exhibited a noted reduction in toe region consistent with a stiffening of material.

Mechanical characterization through biaxial tensile testing of samples after induced stretch shows that GLUT BP stiffened significantly after stretching in both the PD and XD direction (Fig. 7a, c). TRI BP did not exhibit this stiffening and exhibited no significant difference in biomechanical behavior after induced stretch in either the PD or XD direction (Fig. 7b, d). TRI BP was able to maintain its more compliant behavior over GLUT BP even after simulated mechanical insult.

Free Amine Content Analysis

Free amine content is indicative of the number of free amine groups in the tissue that are not crosslinked and it can depict degradation of crosslinked bonds after fatigue. GLUT BP showed a significantly increased percent free amine content than TRI BP when patches were subjected to static strain testing for 4 weeks (15.7% ± 3.70 and −2.0% ± 3.35, respectively). The increased free amine in GLUT BP suggests that during the period of induced static strain, previously crosslinked amine groups became free within the ECM most likely due to the reversibility of glutaraldehyde crosslinking.

Resistance to In Vivo Calcification and Structural Degradation in vivo

Cellular infiltration, encapsulation, capsule layer thickness, and cellular populations based on morphology were similar in both GLUT and TRI groups after 30 days of implantation suggesting that they have similar biocompatibility (Fig. 8a, c). Immunostaining with CD68 showed that macrophages were present around and inside the implant after 30 days implantation in both GLUT and TRI BP (data not shown).

Alizarin red staining on GLUT BP showed heavy calcification after 30 days implantation (Fig. 8b). Alizarin red staining on TRI-treated leaflets showed no calcification after implantation (Fig. 8d). This is consistent with quantitative mineral analysis on explanted

GLUT or TRI BP which indicated significantly more calcium (120.7 ± 18.34 and 25.3 ± 2.98 μg/mg dry tissue, respectively; Fig. 8e) and phosphorus (70.3 ± 3.44 and 14.3 ± 1.47 μg/mg dry tissue, respectively; Fig. 8e) content in GLUT BP compared to TRI BP.

Explants were also analyzed histologically for ECM degradation. Masson's VVG stain did not exhibit clearly defined black, purple elastin fibrous network in GLUT BP explants suggesting that elastin was not stabilized and thus degraded during implantation (Fig. 8f). However, black, purple elastin fibrous network was retained in TRI BP explants suggesting that elastin was stabilized and thus not degraded during implantation (Fig. 8g).

Discussion

The durability of a BHV design is dependent on its ability to resist chemical, biological, and mechanical insult over time. Therefore, durability is fundamentally underpinned by the method in which an ECM is crosslinked for BHV production. The chemical structure of the crosslinks inherently controls the network structure and stability of the bonds. The three component crosslinking in TRI allows better stabilization (Fig. 1) and it echoes into improved macro-scale material properties in biomechanical behavior.

Efficacy in Stabilizing Major ECM Components Against Enzymatic Degradation

Both GLUT and TRI exhibited similar denaturing (shrink) temperatures around 90 °C; this is indicative of adequate crosslinking of collagen [32]. This was to be expected because both crosslinking chemistries were previously demonstrated to effectively stabilize collagen, a major tissue ECM component. Collagenase challenge also did not degrade tissue in both groups which is consistent with adequate collagen stabilization (Fig. 2).

On the other hand, GLUT did not provide any stabilization for elastin and GLUT BP samples had noticeable elastin degradation during in vitro enzymatic challenge as well as during in vivo implantation (Figs. 2, 3a, c, and 8e). GLUT BP exhibited significant amount of GAG loss after treatment with GAGases while TRI did not. This was consistent with previous studies showing that TRI treatment prevented GAG loss in porcine aortic valve leaflets [45]. However, the amount of GAGs present in BP samples is minuscule and we did not find any noticeable change in resistance to tearing (Fig. 4). Previous studies with porcine aortic heart valve leaflets showed decrease in bending stiffness after 10 million cycles of in vitro fatigue [32], thus the effect of GAG loss on long-term fatigue of BP samples need to be tested. Because GAGs are acting as bridges between collagen bundles, the loss of GAGs could cause more voids and sites for calcification. Therefore, stabilizing all components of the ECM may prove beneficial long-term.

Current testing standards in durability only consider accelerated wear testing at 200MIL+ cycles in saline of buffer solutions as demonstration of durability; however, ECM fragmentation from biological enzyme insult can also drastically affect durability. It is important to note ECM fragmentation can elicit oxidative stress and upregulate inflammation responses [46]. Because ECM fragmentation both modulates the intensity of the host cellular response and the physical biomechanics of the ECM, it is paramount that

we consider stabilization of all major ECM components in developing novel methods of producing biomaterials for BHVs.

Strength of GLUT vs TRI Biomaterials

TRI BP required more tearing stress to cause rupture in the material than GLUT BP (Fig. 4). Results were consistent with the previous study with PAVs [45]. BP inherently has more collagen content than PAV, which explains large increase in material strength when comparing BP and PAV leaflets.

TRI BP was expected to be stronger than GLUT BP because the higher crosslinking network of TRI due to chain extending at neomycin nodes (Fig. 1). The combination approach that utilizes irreversible carbodiimide chemistry extended network to form a tighter mesh and incorporation of additional agents for stabilization results in a stronger bio-material. Fabricating a biomaterial that can withstand more stress before tearing is critical in developing a more durable BHV biomaterial because 30% of failed BP BHVs exhibit tearing without calcification at the suture points [28].

Tissue Compliance and Permanent Set in GLUT-and TRI-Fixed Biomaterials

Mechanical characterization data shows that the TRI BP is more compliant than the GLUT BP (Fig. 6). This seems to be on the contrary to our previous mechanical study of the TRI-fixed porcine aortic valves [45]. This is likely due to the differences in ECM composition of the two tissues, where BP has significantly lower elastin and GAGs content. Due to the lower content of elastin and thus tissue recoil property, BP is less compliant than PAV. The loss of elastin and GAGs during GLUTcrosslinking process may cause tissue deformation during crosslinking. This effect is also similar to that of the pressure fixation [6], where the material can become stiffer when fixed in an extended state. TRI, which better stabilizes the ECM and enhances the response of the toe region (specifically from stability of elastin), may have resisted this deformation during crosslinking. Thus this observed compliance of TRI BP may be additional evidence of the fixation of ECM components in native tissue like state.

GLUT BP showed extensive deformation due to permanent set during static strain experiment (Figs. 5 and 7a, c). The TRI treatment showed no statistical difference with the non-extended directions. We observed slight deformation as a result of the flattening of the tissue underneath the clamps. This artifactual deformation may be partially responsible for the observed small deformation of the TRI. Thus, the ability of the TRI method to resist permanent set may be better than the results indicate. The lack of directional differences is as expected (Table 1). The strains observed for the permanent set is in the toe region where no collagen fibers are straightened. Therefore, the mechanical response in this region is mainly determined by the non-fibrous matrix, which based on our current understanding is essentially isotropic. As such, permanent set is also expected to be isotropic, which also offers greater emphasis on stabilizing the non-collagenous matrix to resist permanent set. It is expected that permanent set effects are minimal (close to ideal) in the direction that was orthogonal to the axis of stretching (direction in which the tissue was not stretched). If a tissue exhibits permanent set, it would be expected to occur in the same direction as

stretching (λ deviates heavily from 1). Minimal shear was observed from the deformation gradient determined from the bilinear interpolation of the markers (<0.02).

Such permanent set in GLUT-fixed tissues has been previously observed in both explanted failed BHVs as well as in vitro fatigue-tested BHVs in which permanent geometric alteration to the tissue itself has caused visible “cusp sagging” with significant disruption to collagen fiber orientation as well as visible damage to the biomaterial [5, 30, 31, 47]. These studies suggest that permanent set predisposes BHVs to premature failure by introducing altered mechanical behavior causing stress concentrations to accrue at weak points in the BHV design. Therefore, preventing permanent set through using a more irreversible chemistry such as TRI could produce a more durable BHV biomaterial long-term. This would slow or even possibly prevent altered stress concentrations to gather at weak points that can cause tearing.

Biaxial tensile testing after static stretch experiment shows that the TRI crosslinking better preserves the mechanical extensibility of the pericardium (Fig. 7b, d) than GLUT (Fig. 7a, c). TRI crosslinking shows an extended toe region in comparison to the GLUT, but the maximum tangent modulus does not appear to be significantly changed. This is opposite of the permanent set results where GLUT showed more permanent set despite being stiffer (Fig. 7a, c).

The instability of glutaraldehyde bonds results in breaking of bonds allowing collagen fibers to slowly lose crimp and set into new orientation as new bonds form. This process repeats over and over again over time and results in loss of extensibility and a creep effect in the biomaterial (Fig. 5). Coupled with degrading ECM proteins, the biomaterial loses its ability to return to its original gauge length and permanently assumes the new length. This result was also corroborated with higher free amine content in GLUT-treated tissue, clearly suggesting breaking of Schiff’s base bonds during stretching. This increase in free amine content could be correlated with permanent set. Increased free amine content is most likely due to decreased crosslinking between collagen fibers thus unstable collagen fibers are unraveling and losing their crimp; coupled with loss of elastin, the entire tissue composite is becoming stiffer and geometrically set into whatever path stress concentrations shunt towards. This does not occur in TRI because the bonds are much more irreversible thereby not allowing the collagen fibers to lose their original positions at the substrate level. The stacked approach with irreversible carbodiimide chemistry in combination with additives also further stabilize entire ECM integrity and does not let the fibers undergo this creep effect thereby preventing permanent set. Because carbodiimide bonds are irreversible, increase in amine content did not occur in TRI-treated samples and we did not find major permanent set in TRI group.

Implications of TRI in Reducing Calcification of BHVs

TRI exhibits four- to sixfold less mineralization than GLUT (Fig. 8b, d, g) which was similar to anti-calcification treatments such as AOA, Thermafix™, Linx™, and alcohol-/ethanol-based approaches have been proven effective to delay the onset of calcification [24] and are currently used clinically. However, all anti-calcification methods studied so far are not directed to prevent mechanical and chemical degeneration of material. No data has been

presented for such anti-calcification treatments that further results in increased mechanical or biological durability. Marginal increases have been made to BHV implant life, if any, since the introduction of these technologies [9, 27, 48].

Carbodiimide and PGG have previously been demonstrated to reduce calcification independently [49–51] and the data in this study suggests that the combined use significantly reduces the calcification process. This is most likely accomplished due to improved ECM stability through highly networked, irreversible chemical crosslinking that prevents ECM fragmentation thereby reducing the availability of high affinity sites for calcification on damaged collagen and elastin.

This added value in mechanical and biological durability merits further long-term fatigue testing for durability and implantation of TRI-treated BHVs as mitral valve replacement in sheep to study calcification and biocompatibility as a blood-contacting device.

Limitations of Study

Static strain was used to quickly investigate the materials' ability to resist permanent geometric deformation. Therefore, we induced the permanent set in the simplest way possible via induced static strain. Long-term cyclic fatigue testing at more physiological conditions is required. We also used enzymatic challenges in vitro to mimic in vivo situations. Our methods may be harsher than what is observed in vivo as we wanted to accelerate the process. Such damage would take multiple years of implantation in vivo. The subdermal calcification study clearly shows that TRI tissues are less prone to calcification; however, we need to test these tissues as heart valve implants in circulatory environment in larger animals to study calcification.

Conclusion

The data suggest that TRI crosslinking may produce a better biomaterial for BHV fabrication because TRI better stabilizes the ECM through irreversible chemistry that prevents micro and macro deformations (preventing permanent set) and higher resistance to tearing, which may be the underlying driver behind structural degradation resulting in mechanical failure. This novel biomaterial also substantially resists calcification. GLUT crosslinking that has been used for several decades exhibited reduced stability in ECM component and permanent set effects due to the reversibility of Schiff's base bond chemistry. TRI is a novel chemical fixation technique that can be adopted by industry to produce more durable BHVs that can be used to expand the market of BHVs for younger populations.

Acknowledgments

Source of Funding: This work was supported by the National Institutes of Health (R01HL108330 and P20GM103444) and Hunter Endowment to NRV.

References

1. Schoen FJ. Evolving concepts of cardiac valve dynamics: the continuum of development, functional structure, pathobiology, and tissue engineering. Circulation. 2008; 118(18):1864–80. [PubMed: 18955677]
2. Manji RA, Menkis AH, Ekser B, Cooper DK. Porcine bioprosthetic heart valves: the next generation. American Heart Journal. 2012; 164(2):177–85. [PubMed: 22877802]
3. Siddiqui RF, Abraham JR, Butany J. Bioprosthetic heart valves: modes of failure. Histopathology. 2009; 55(2):135–44. [PubMed: 19694820]
4. Mohammadi H, Mequanint K. Prosthetic aortic heart valves: modeling and design. Medical Engineering and Physics. 2011; 33(2):131–47. [PubMed: 20971672]
5. Sacks MS, Schoen FJ. Collagen fiber disruption occurs independent of calcification in clinically explanted bioprosthetic heart valves. Journal of Biomedical Materials Research. 2002; 62(3):359–71. [PubMed: 12209921]
6. Wells SM, Sellaro T, Sacks MS. Cyclic loading response of bioprosthetic heart valves: effects of fixation stress state on the collagen fiber architecture. Biomaterials. 2005; 26(15):2611–9. [PubMed: 15585264]
7. Eckert CE, Fan R, Mikulis B, Barron M, Carruthers CA, Friebe VM, Vyavahare NR, Sacks MS. On the biomechanical role of glycosaminoglycans in the aortic heart valve leaflet. Acta Biomaterialia. 2013; 9(1):4653–60. [PubMed: 23036945]
8. Sacks MS, David Merryman W, Schmidt DE. On the biomechanics of heart valve function. Journal of Biomechanics. 2009; 42(12):1804–24. [PubMed: 19540499]
9. Zilla P, Brink J, Human P, Bezuidenhout D. Prosthetic heart valves: catering for the few. Biomaterials. 2008; 29(4):385–406. [PubMed: 17950840]
10. Aslam AK, Aslam AF, Vasavada BC, Khan IA. Prosthetic heart valves: types and echocardiographic evaluation. International Journal of Cardiology. 2007; 122(2):99–110. [PubMed: 17434628]
11. Takkenberg JJ, van Herwerden LA, Eijkemans MJ, Bekkers JA, Bogers AJ. Evolution of allograft aortic valve replacement over 13 years: results of 275 procedures. European Journal of Cardio-Thoracic Surgery Official Journal of the European Association for Cardio-Thoracic Surgery. 2002; 21(4):683–91. discussion 691. [PubMed: 11932168]
12. Schoen FJ, Tsao JW, Levy RJ. Calcification of bovine pericardium used in cardiac valve bioprostheses. Implications for the mechanisms of bioprosthetic tissue mineralization. The American Journal of Pathology. 1986; 123(1):134–45. [PubMed: 2421577]
13. Schoen FJ, Levy RJ, Nelson AC, Bernhard WF, Nashef A, Hawley M. Onset and progression of experimental bioprosthetic heart valve calcification. Laboratory Investigation A Journal of Technical Methods and Pathology. 1985; 52(5):523–32. [PubMed: 3990244]
14. Strates, LJB., Nimni, ME. Calcification in cardiovascular tissues and bioprostheses. Bova Rotan: CRC Press; 1989. Biotechnology ed
15. Rucker RB. Calcium binding to elastin. Adv Exp Med Biol. 1974; 48:185–209. [PubMed: 4372871]
16. Perrotta I, Russo E, Camastra C, Filice G, Di Mizio G, Colosimo F, Ricci P, Tripepi S, Amorosi A, Triumbari F, Donato G. New evidence for a critical role of elastin in calcification of native heart valves: immunohistochemical and ultrastructural study with literature review. Histopathology. 2011; 59(3):504–13. [PubMed: 22034890]
17. Gott JP, Girardot MN, Girardot JM, Hall JD, Whitlark JD, Horsley WS, Dorsey LM, Levy RJ, Chen W, Schoen FJ, Guyton RA. Refinement of the alpha aminooleic acid bioprosthetic valve anticalcification technique. The Annals of Thoracic Surgery. 1997; 64(1):50–8. [PubMed: 9236334]
18. Ogle MF, Kelly SJ, Bianco RW, Levy RJ. Calcification resistance with aluminum-ethanol treated porcine aortic valve bioprostheses in juvenile sheep. The Annals of Thoracic Surgery. 2003; 75(4): 1267–73. [PubMed: 12683574]
19. Levy RJ, Vyavahare N, Ogle M, Ashworth P, Bianco R, Schoen FJ. Inhibition of cusp and aortic wall calcification in ethanol- and aluminum-treated bioprosthetic heart valves in sheep:

background, mechanisms, and synergism. The Journal of Heart Valve Disease. 2003; 12(2):209–16. discussion 216. [PubMed: 12701794]

20. Vyavahare N, Hirsch D, Lerner E, Baskin JZ, Schoen FJ, Bianco R, Kruth HS, Zand R, Levy RJ. Prevention of bioprosthetic heart valve calcification by ethanol preincubation. Efficacy and Mechanisms, Circulation. 1997; 95(2):479–88. [PubMed: 9008467]
21. Trantina-Yates AE, Human P, Zilla P. Detoxification on top of enhanced, diamine-extended glutaraldehyde fixation significantly reduces bioprosthetic root calcification in the sheep model. The Journal of Heart Valve Disease. 2003; 12(1):93–100. discussion 100–1. [PubMed: 12578343]
22. Zilla P, Bezuidenhout D, Weissenstein C, van der Walt A, Human P. Diamine extension of glutaraldehyde crosslinks mitigates bioprosthetic aortic wall calcification in the sheep model. Journal of Biomedical Materials Research. 2001; 56(1):56–64. [PubMed: 11309791]
23. Bezuidenhout D, Oosthuysen A, Human P, Weissenstein C, Zilla P. The effects of cross-link density and chemistry on the calcification potential of diamine-extended glutaraldehyde-fixed bioprosthetic heart-valve materials. Biotechnology and Applied Biochemistry. 2009; 54(3):133–40. [PubMed: 19882764]
24. Wright G, de la Fuente A. Effectiveness of anti-calcification technologies in a rabbit model. The Journal of Heart Valve Disease. 2015; 24(3):386–92. [PubMed: 26901918]
25. Zilla P, Weissenstein C, Bracher M, Human P. The anticalcific effect of glutaraldehyde detoxification on bioprosthetic aortic wall tissue in the sheep model. Journal of Cardiac Surgery. 2001; 16(6):467–72. [PubMed: 11925027]
26. Shang H, Claessens SM, Tian B, Wright GA. Aldehyde reduction in a novel pericardial tissue reduces calcification using rabbit intramuscular model. Journal of Materials Science Materials in Medicine. 2017; 28(1):16. [PubMed: 28000112]
27. Chiang YP, Chikwe J, Moskowitz AJ, Itagaki S, Adams DH, Egorova NN. Survival and long-term outcomes following bioprosthetic vs mechanical aortic valve replacement in patients aged 50 to 69 years. JAMA. 2014; 312(13):1323–9. [PubMed: 25268439]
28. Singhal P. Bioprosthetic heart valves: impact of implantation on biomaterials. ISRN Biomaterials. 2013; 2013:1–16.
29. Sellaro TL, Hildebrand D, Lu Q, Vyavahare N, Scott M, Sacks MS. Effects of collagen fiber orientation on the response of biologically derived soft tissue biomaterials to cyclic loading. Journal of Biomedical Materials Research Part A. 2007; 80(1):194–205. [PubMed: 17041913]
30. Sun W, Sacks M, Fulchiero G, Lovekamp J, Vyavahare N, Scott M. Response of heterograft heart valve biomaterials to moderate cyclic loading. Journal of Biomedical Materials Research Part A. 2004; 69(4):658–69. [PubMed: 15162408]
31. Smith DB, Sacks MS, Pattany PM, Schroeder R. High-resolution magnetic resonance imaging to characterize the geometry of fatigued porcine bioprosthetic heart valves. The Journal of Heart Valve Disease. 1997; 6(4):424–32. [PubMed: 9263876]
32. Vyavahare N, Ogle M, Schoen FJ, Zand R, Gloeckner DC, Sacks M, Levy RJ. Mechanisms of bioprosthetic heart valve failure: fatigue causes collagen denaturation and glycosaminoglycan loss. Journal of Biomedical Materials Research. 1999; 46(1):44–50. [PubMed: 10357134]
33. Scott M, Vesely I. Aortic valve cusp microstructure: the role of elastin. The Annals of Thoracic Surgery. 1995; 60(2 Suppl):S391–4. [PubMed: 7646194]
34. Lee TC, Midura RJ, Hascall VC, Vesely I. The effect of elastin damage on the mechanics of the aortic valve. Journal of Biomechanics. 2001; 34(2):203–10. [PubMed: 11165284]
35. Vesely I. The role of elastin in aortic valve mechanics. Journal of Biomechanics. 1998; 31(2):115–23. [PubMed: 9593204]
36. Christian AJ, Lin H, Alferiev IS, Connolly JM, Ferrari G, Hazen SL, Ischiropoulos H, Levy RJ. The susceptibility of bioprosthetic heart valve leaflets to oxidation. Biomaterials. 2014; 35(7): 2097–102. [PubMed: 24360721]
37. Sacks MS. The biomechanical effects of fatigue on the porcine bioprosthetic heart valve. Journal of Long-Term Effects of Medical Implants. 2001; 11(3–4):231–47. [PubMed: 11921666]
38. Tripi DR, Vyavahare NR. Neomycin and pentagalloyl glucose enhanced cross-linking for elastin and glycosaminoglycans preservation in bioprosthetic heart valves. Journal of Biomaterials Applications. 2014; 28(5):757–66. [PubMed: 24371208]

39. Yang B, Lesicko J, Sharma M, Hill M, Sacks MS, Tunnell JW. Polarized light spatial frequency domain imaging for non-destructive quantification of soft tissue fibrous structures. Biomedicals Optics Express. 2015; 6(4):1520–33.
40. Grashow JS, Yoganathan AP, Sacks MS. Biaxial stress-stretch behavior of the mitral valve anterior leaflet at physiologic strain rates. Annals of Biomedical Engineering. 2006; 34(2):315–25. [PubMed: 16450193]
41. Zhang W, Feng Y, Lee CH, Billiar KL, Sacks MS. A generalized method for the analysis of planar biaxial mechanical data using tethered testing configurations. Journal of Biomechanical Engineering. 2015; 137(6):064501. [PubMed: 25429606]
42. Billiar KL, Sacks MS. Biaxial mechanical properties of the natural and glutaraldehyde treated aortic valve cusp—part I: experimental results. Journal of Biomechanical Engineering. 2000; 122(1):23–30. [PubMed: 10790826]
43. Gratzer PF, Lee JM. Control of pH alters the type of cross-linking produced by 1-ethyl-3-(3-dimethylaminopropyl)-carbodiimide (EDC) treatment of acellular matrix vascular grafts. Journal of Biomedical Materials Research. 2001; 58(2):172–9. [PubMed: 11241336]
44. Olde Damink LH, Dijkstra PJ, van Luyn MJ, van Wachem PB, Nieuwenhuis P, Feijen J. Cross-linking of dermal sheep collagen using a water-soluble carbodiimide. Biomaterials. 1996; 17(8): 765–73. [PubMed: 8730960]
45. Tam H, Zhang W, Feaver KR, Parchment N, Sacks MS, Vyavahare N. A novel crosslinking method for improved tear resistance and biocompatibility of tissue based biomaterials. Biomaterials. 2015; 66:83–91. [PubMed: 26196535]
46. Trantina-Yates A, Weissenstein C, Human P, Zilla P. Stentless bioprosthetic heart valve research: sheep versus primate model. The Annals of Thoracic Surgery. 2001; 71(5 Suppl):S422–7. [PubMed: 11388240]
47. Martin C, Sun W. Modeling of long-term fatigue damage of soft tissue with stress softening and permanent set effects. Biomechanics and Modeling in Mechanobiology. 2013; 12(4):645–55. [PubMed: 22945802]
48. Zilla P, Human P, Bezuidenhout D. Bioprosthetic heart valves: the need for a quantum leap. Biotechnology and Applied Biochemistry. 2004; 40(Pt 1):57–66. [PubMed: 15270708]
49. Girardot JM, Girardot MN. Amide cross-linking: an alternative to glutaraldehyde fixation. The Journal of Heart Valve Disease. 1996; 5(5):518–25. [PubMed: 8894992]
50. Isenburg JC, Karamchandani NV, Simionescu DT, Vyavahare NR. Structural requirements for stabilization of vascular elastin by polyphenolic tannins. Biomaterials. 2006; 27(19):3645–51. [PubMed: 16527345]
51. Chow JP, Simionescu DT, Warner H, Wang B, Patnaik SS, Liao J, Simionescu A. Mitigation of diabetes-related complications in implanted collagen and elastin scaffolds using matrix-binding polyphenol. Biomaterials. 2013; 34(3):685–95. [PubMed: 23103157]

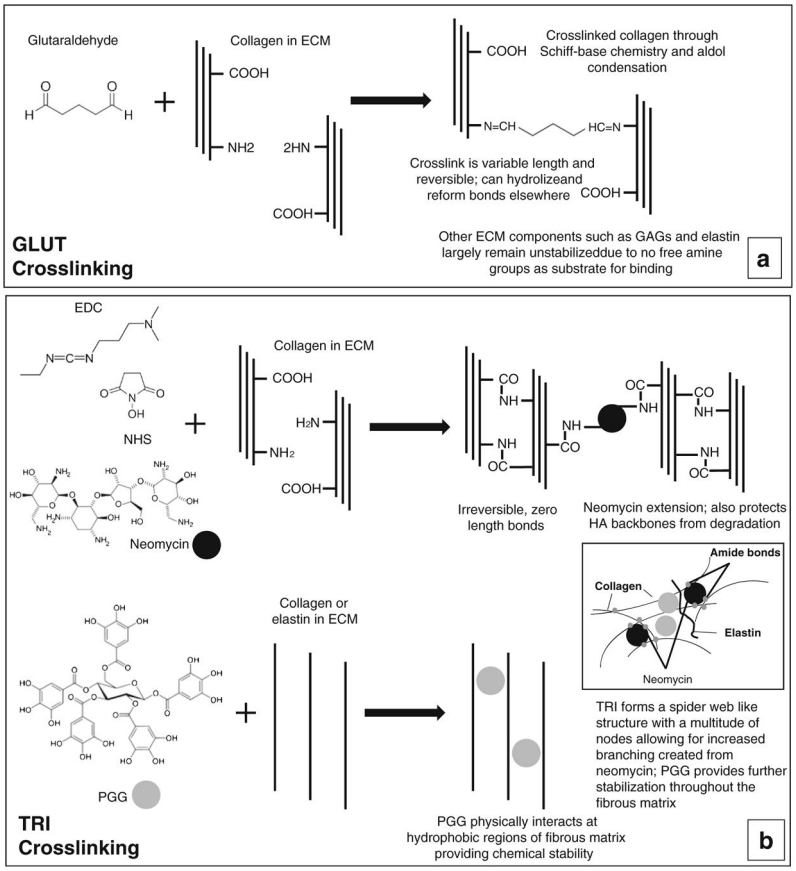

Fig. 1.

Crosslinking chemistry of bovine pericardium (BP). **a** Glutaraldehyde crosslinking mechanism. **b** Combined crosslinking (TRI) that incorporates EDC + NHS (carbodiimide crosslinking), neomycin, and pentagalloyl glucose (PGG). *Inset* depicts TRI stabilization of collagen, GAGs, and elastin throughout the entire ECM tissue composite of BP

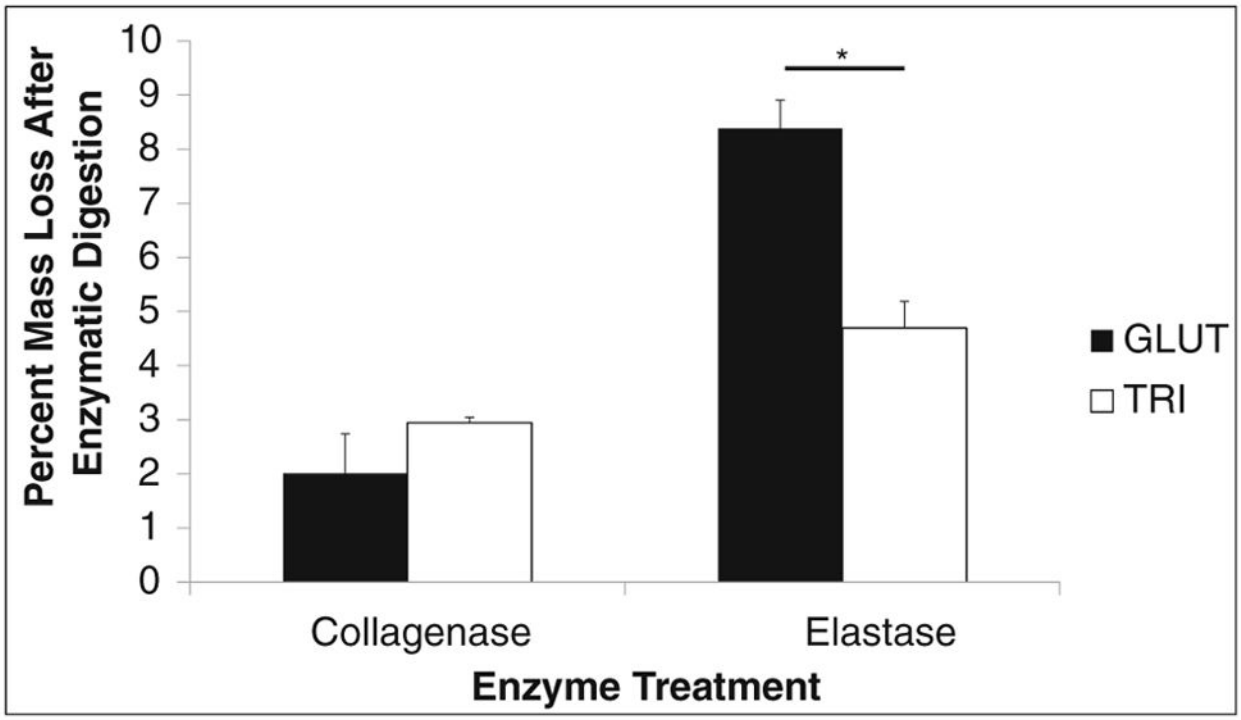

Fig. 2.

Percent mass loss before and after collagenase or elastase treatment of GLUT or TRI BP. *Asterisk* indicates significant difference ($p < 0.05$)

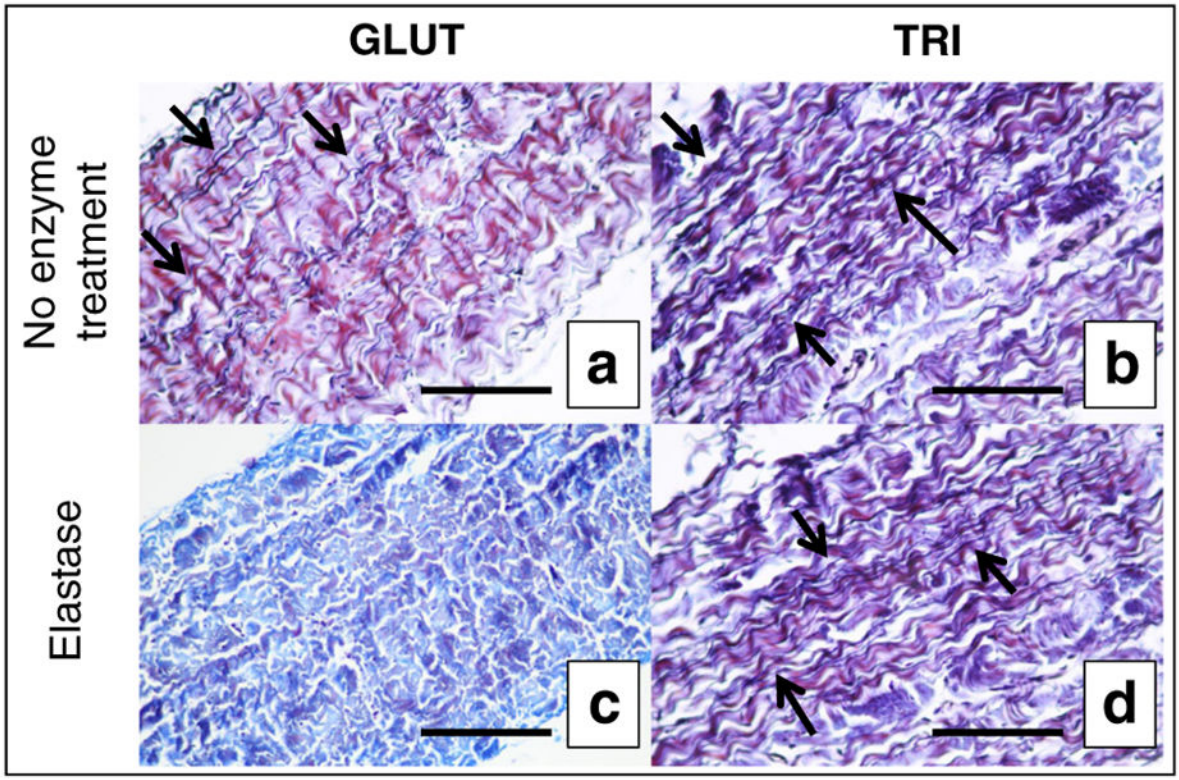

Fig. 3.

Histological evaluation of collagen and elastin stability in vitro in GLUT or TRI BP stained with combined Verhoeff's elastic Masson's trichrome method. **a** GLUT BP after crosslinking. **b** TRI BP after crosslinking. **c** GLUT BP after 60 days' storage + elastase treatment. **d** TRI BP after 60 days' storage + elastase treatment. *Black scale bars* represent 200 μm

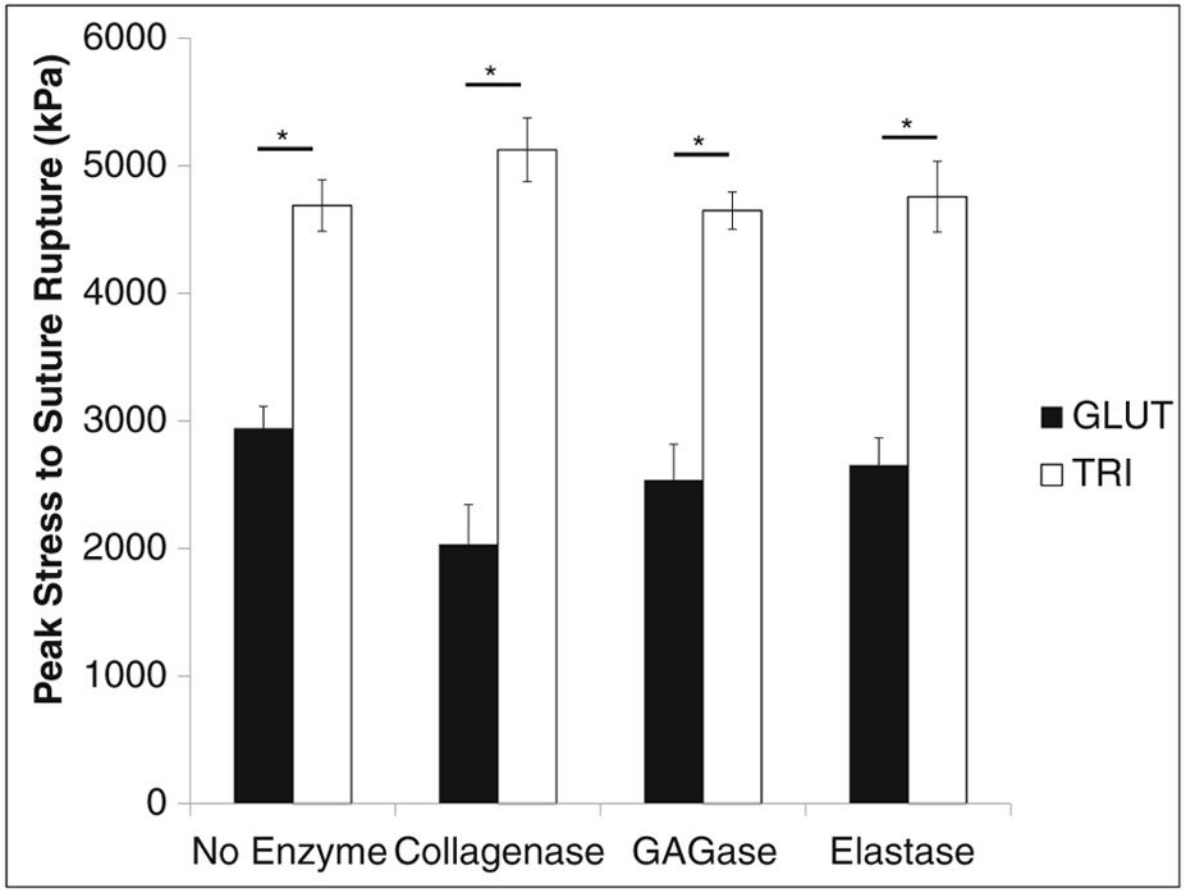

Fig. 4.

Peak stress to cause rupture in GLUT or TRI BP materials treated with collagenase, elastase, or GAGase. *Asterisk* indicates significant difference ($p < 0.05$)

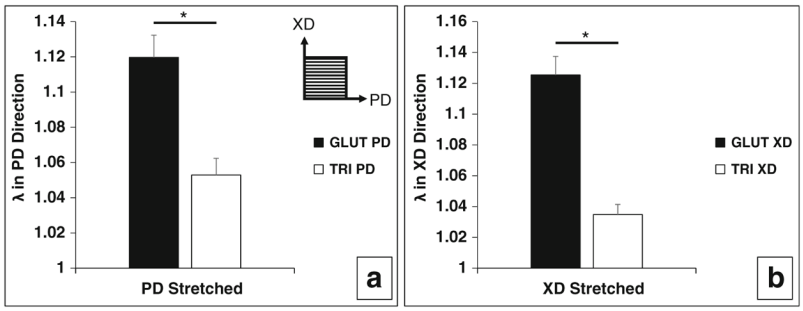

Fig. 5.

Geometric dimensional changes in GLUT- or TRI-treated BP patches in preferred orientation (PD—along collagen alignment) or non-preferred direction (XD—against collagen alignment) after induced static strain testing. **a** Permanent set induced in PD direction of GLUT- or TRI-treated BP patches from stretching in PD direction. **b** Permanent set induced in XD direction of GLUT- or TRI-treated BP patches from stretching in XD direction. $\lambda = 1$ is indicative of no change in geometric dimensions (no factor change in gauge length before and after induced static strain testing). *Asterisk* indicates significant difference ($p < 0.05$)

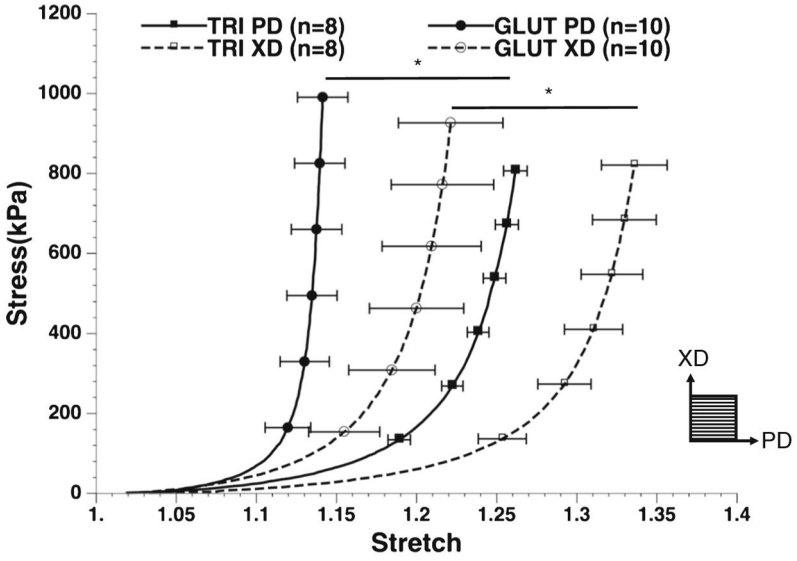

Fig. 6.

Biaxial tensile testing of GLUT or TRI BP in preferred (PD—with collagen alignment) or non-preferred (XD—orthogonal to collagen alignment) direction before induced static strain

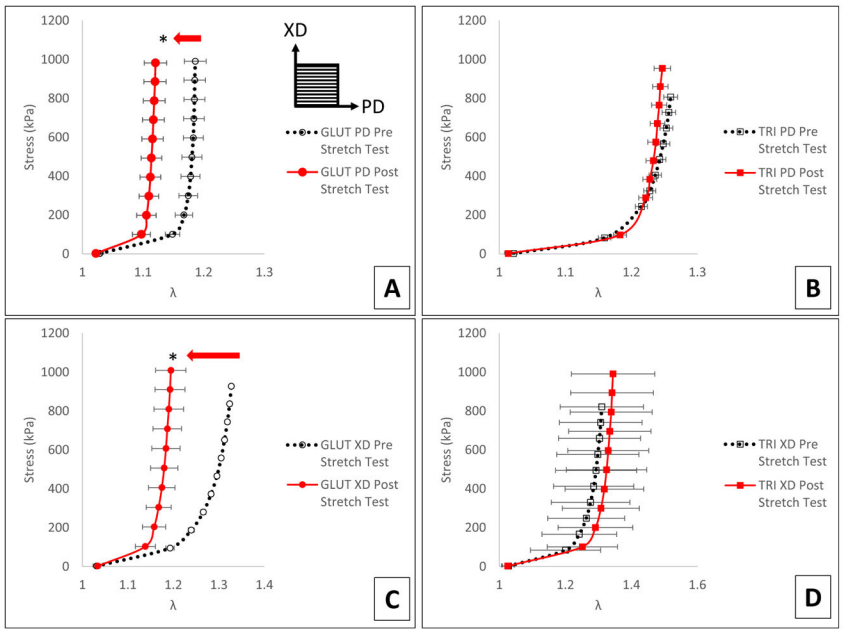

Fig. 7.

Apparent mechanical behavior of GLUT or TRI BP before and after induced static strain. **a** GLUT BP biaxial tensile testing of PD direction before and after induced static strain in PD direction. **b** TRI BP biaxial tensile testing of PD direction before and after induced static strain in PD direction. **c** GLUT BP biaxial tensile testing of XD direction before and after induced static strain in XD direction. **d** TRI BP biaxial tensile testing of XD direction before and after induced static strain in XD direction. *Arrow* indicates significant shift in biomechanical behavior after induced strain. Orientation of PD and XD directions are indicated in **a**. *Asterisk* indicates significant difference ($p < 0.05$)

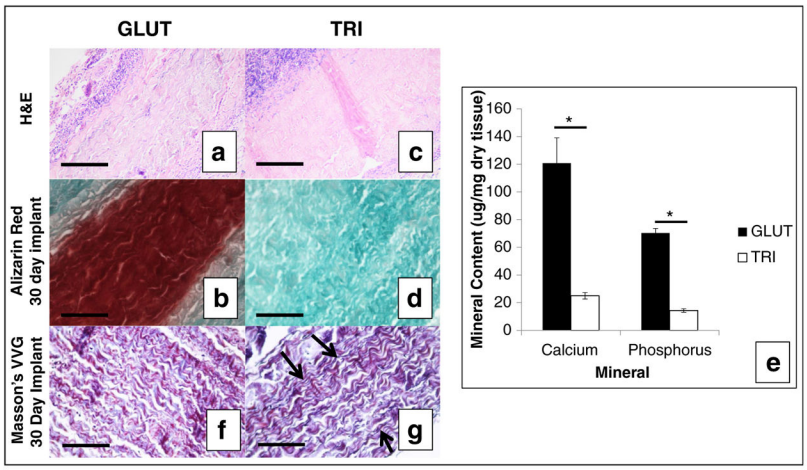

Fig. 8.

Histological assessment of GLUT or TRI BP after 30 days in vivo implantation. **a**, **c** *H&E* stain. **b**, **d** Alizarin *red* stain and counterstained with *green* for calcium. **e**, **f** Masson's VVG stain, *black arrows* indicate *dark black* to *purple fibers* of elastin. Collagen is stained *dark blue* or *purple; scale bars* represent 200 μm. **g** Quantitative mineral content in explanted BP patches. *Asterisk* indicates significant difference ($p < 0.05$)

Table 1

Permanent geometric deformation results from induced static strain on GLUT or TRI BP patches

	Change in length in PD direction λ_{PD}	SEM_{PD}	Change in length in XD direction λ_{XD}	SEM_{XD}
Stretched in PD direction				
GLUT (n=3)	**1.1197**	**0.0126**	1.0356	0.0125
TRI (n = 5)	**1.0529**	**0.0095**	1.0377	0.0195
Stretched in XD direction				
GLUT (n = 7)	1.0281	0.0156	**1.1254**	**0.0121**
TRI (n = 3)	1.0449	0.0095	**1.0348**	**0.0066**

Bolded values are changes in gauge length in the direction of induced static strain. Unbolded values are changes in length orthogonal to the direction of induced static strain